

Supporting Information

Contents

- 1. General Remarks**
- 2. Synthesis of ionic liquids**
- 3. Mechanism confirmation (MS & simulation)**
- 4. General procedure for coupling reaction between PO and
CH₃OH**

1. General Remarks

N, N-diethyl-4-nitroaniline (P1), 4-nitroaniline (P2) and 2,6-dichloro-4-(2,4,6-triphenyl-1-pyridino)-phenolate (Reichardt's dye 33, P3), NaOH triethylamine and imidazole were purchased from Aladdin. [N₂₂₂₂][AC] were purchased from Lanzhou Institute of Chemical Physics, Chinese Academy of Sciences. After washing by diethyl ether three times, the ILs were dried under high vacuum (10⁻³ Pa) at 50 °C for 24 h. ILs were characterized by ¹H NMR spectroscopy in DMSO-d₆ using a JNM-ECA 600 MHz nuclear magnetic resonance (NMR) spectrometer to determine their structures.

¹H NMR ([N₂₂₂₂][OAC], DMSO): 1.15 (t, 12H), 1.54 (s, 3H), 3.22 (m, 8H)

2. Synthesis of ionic liquids

Synthesis of Triethylmethylammonium methylcarbinolate ([N₂₂₂₁][MC]) : The preparation of [N₂₂₂₁][MC] was following representative procedure: Firstly, triethylamine (1.4 g), dimethylcarbonate (3.6 g) and methanol (5 ml) were mixed in a micro wave reaction tube at 393.15 K for 6 h with magnetic stirring. After the reaction, the mixture was dried by reduced pressure distillation, then, the resultant solution was washed with hexane three times to remove redundant DMC and trimethylamine that did not react. After that, the resultant was dried under high vacuum (10⁻³Pa) at 323k for 24h.

¹H NMR (700MHZ, DMSO): δ/ppm=1.2 (t, 9H), 2.9 (s, 3H), 2.97-3.27 (s and m, 9H).

ESI-MS: +ve mode:116.14 ([C₇H₁₈N]); -ve mode:75.05 ([C₂H₃O₃]).

3. Mechanism confirmation

Experimental

Several experiments were taken to verify the mechanism by Bruker QTOF II Mass Spectrometry (ESI-QTOF-MS):

1) PO reacted with ILs

The desired amount of PO and ILs ($[N_{2221}][MC]$ or $[N_{2222}][AC]$) were taken into autoclave reactor at 80 °C for 30 min. The solution change from two phase to a homogeneous one after reaction ($[N_{2222}][AC]$ can be show in Figure S1). Further, the resultant was test by ESI-QTOF-MS in positive ion mode and negative ion mode. (Figure S2-S3)

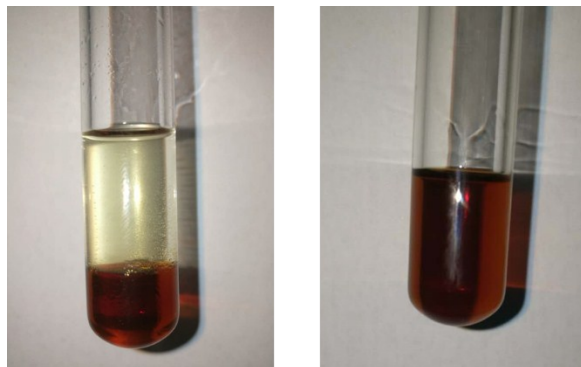


Figure S1: Images of $[N_{2222}][AC]$ and PO before and after the reaction

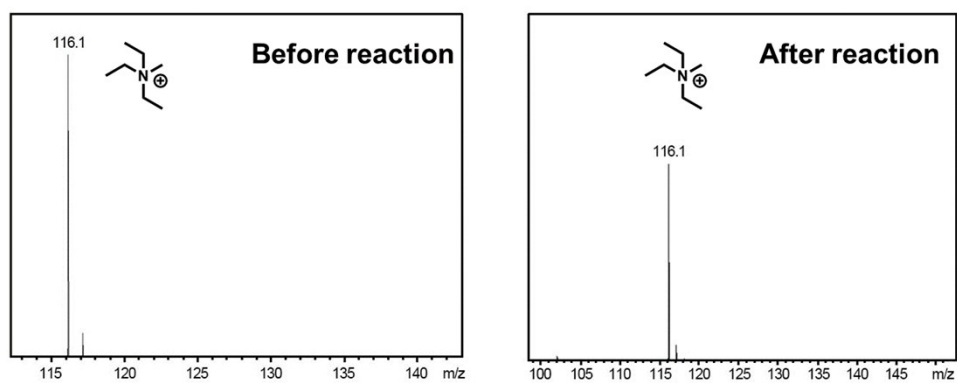


Figure S2: ESI-QTOF-MS of positive ion sample before and after 30 min for reaction of PO and $[N_{2221}][MC]$

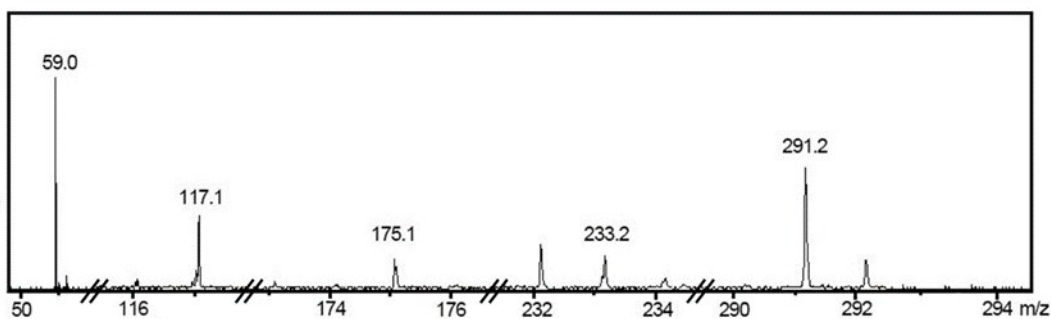


Figure S3: ESI-QTOF-MS of negative ion sample after the reaction of PO and $[N_{2222}][AC]$

2) Reactivity of ILs during the coupling reaction of PO and methanol

The experiments were carried out a 100 ml autoclave reactor. PO, CH₃OH and ILs (PO 0.25 mol, CH₃OH 0.75 mol, [N₂₂₂₁][MC] 0.25 mmol) were introduced into reactor (100 ml). After running at 80°C for 30 min, the reactor was cooled down to room temperature with the product analyzed by ESI-QTOF-MS in negative ion mode (Figure S4).

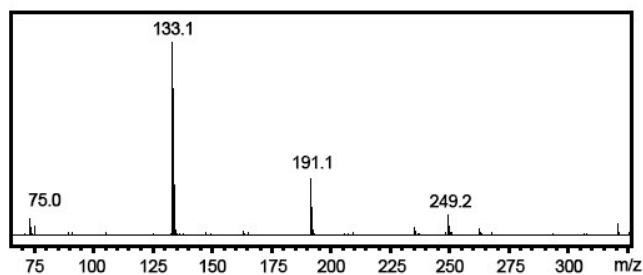


Figure S4: ESI-QTOF-MS of negative ion sample after 30 min for reaction of PO and methanol catalyzed by [N₂₂₂₁][MC]

3) Measurement of Kamlet-Taft parameters

The reactant from [N₂₂₂₁][MC] (MC-ILs1) and PO was extracted and distilled by n-hexane after reaction at 80°C for 30 min to obtain the reactive ILs (MC-ILs-n).

Then, Individual stock solution of the dyes P1, P2 and P3 were prepared in dichloromethane (DCM). An appropriate volume of stock solution was added to MC-ILs1 and MC-ILs-n (dye/IL, ca. 0.5 mM). The samples were then under vacuum to remove residual DCM at 30 °C for 12 h. The dried dye/IL solution was then added to a cuvette analyzed by UV-Vis spectrum of all samples at room temperature using a PC-controlled SHIMADZU UV-1700

PaharmaSpec Spectrophotometer.

The solvatochromic probe analysis was introduced by Kamlet-Taft linear solvation energy relationship composed of the complimentary scales of hydrogen bond donating ability (α), hydrogen bond accepting ability (β), and dipolarity/polarizability (π^*). Thereinto, the π^* parameter is determined from the spectroscopic shift of P1 using eq. 1.

$$\nu(P1)_{max} = 27.52 - 3.182\pi^* \quad (1)$$

The β parameter is determined using shift of P2 with respect to P1 and eq. 2.

$$\nu(P1)_{max} = 1.035\nu(P1)_{max} - 2.80\beta + 2.64 \quad (2)$$

The ET (30) parameter is determined based on the maximum wavelength of P3 as defined by eq. 3.

$$E_T(30) = 0.9986(28592/\lambda_{\max}(P3)) - 8.6878 \quad (3)$$

The parameter α can then be calculated by using ET (30) with respect to π^* from eq. 4.

$$\alpha = 0.0649E_T(30) - 2.03 - 0.72\pi^* \quad (4)$$

Table S1: Kamlet-Taft parameters of ILs using the following set of dyes: N, N-diethyl-4-nitroaniline, 4-nitroaniline and Reichardt's dye

Cat.	$E_T(30)$	π^*	α	β
MC-ILs1	48.42	1.09	0.33	0.78
MC-ILs-n	48.65	0.29	0.92	1.71

4) Reaction kinetics of NaOH and MC-ILs1

The coupling reaction of PO and methanol catalyzed by [N₂₂₁][MC] were carried out in the microwave reactor under different temperature compared with NaOH. The product was analyzed by a gas chromatograph with FID. Then, the linear fitting was made by eq. 5, where C_{A0} is the concentration of PO initially and x is the conversion of PO, to define the order of reaction.

$$\frac{1}{n-1} \left(\frac{1}{C_A^{n-1}} - \frac{1}{C_{A0}^{n-1}} \right) = kt \rightarrow \frac{1}{n-1} \left(\frac{1}{C_{A0}^{n-1}(1-x)^{n-1}} - \frac{1}{C_{A0}^{n-1}} \right) = kt \quad (5)$$

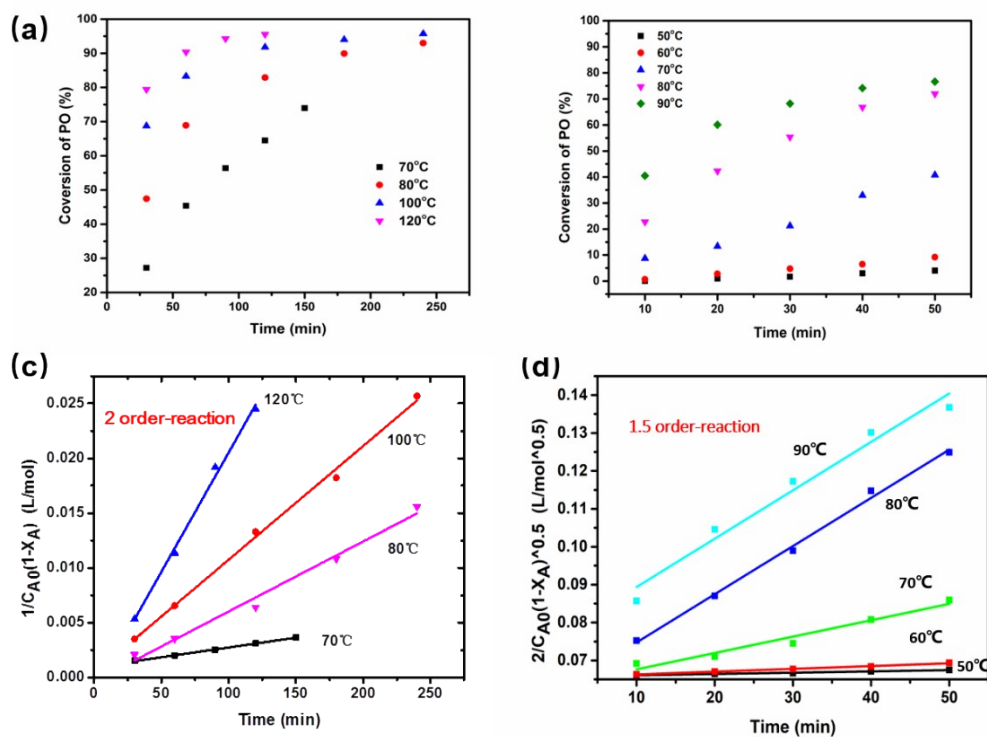


Figure S5: Results of the coupling reaction of PO and methanol under different temperature (a) catalyzed by NaOH, (b) catalyzed by MC-ILs1, and reacton order with (c) NaOH, (d) MC-ILs1

Simulation

All computed thermochemistry and reaction pathway data reported herein are based on gas-phase electronic structure calculations, using Gaussian 16 at the DFT B3LYP/6-311+G(d,p) theory level with Grimme's D3 dispersion corrections.

1) Reaction process of MC-ILs1 with PO

The reaction process was simulated under methanol solvent effect and without solvent effect. The contrast of TS1, TS2, TS3, TS4 and MC-ILs1, MC-ILs2, MC-ILs3, MC-ILs4 indicated that methanol solvent lower the barriers of ring-opening of PO making the reaction kinetics favorable, but the reaction run easily for thermodynamics without solvent effect (Figure S6).

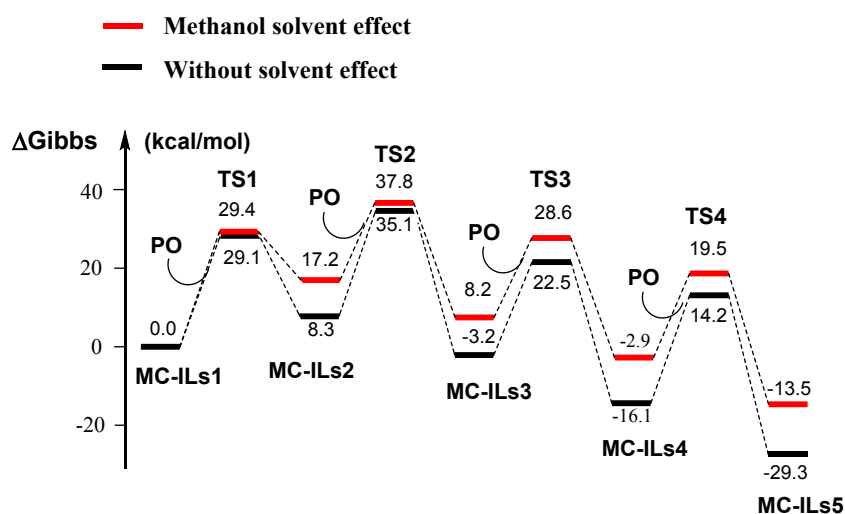


Figure S6: Potential energy profiles for the coupling reaction between MC-ILs1 and PO. Red line represents methanol solvent effect as black for without solvent effect.

2) Reaction process of AC-ILs1 with PO

The ring-opening of PO is promoted both the electrophilic attack of the H atom from [N₂₂₂₂] and the nucleophilic attack from [AC] to form transition state (TS1). After cleavage of C-O, C atom from PO bond to O atom from [AC] as an intermediate (AC-IL2) which can further electrophilic and nucleophilic attack on PO following the above steps with series transition states (TS2, TS3, TS4) and intermediates (AC-IL3, AC-IL4, AC-IL5). The reaction pathway has a lower energy barrier of each ring-opening steps in methanol solvent because of the hydrogen-bond donor surroundings that methanol provided. Compared with methanol effect, the reaction is more favorable in thermodynamics due to the stable intermediates without solvent effect

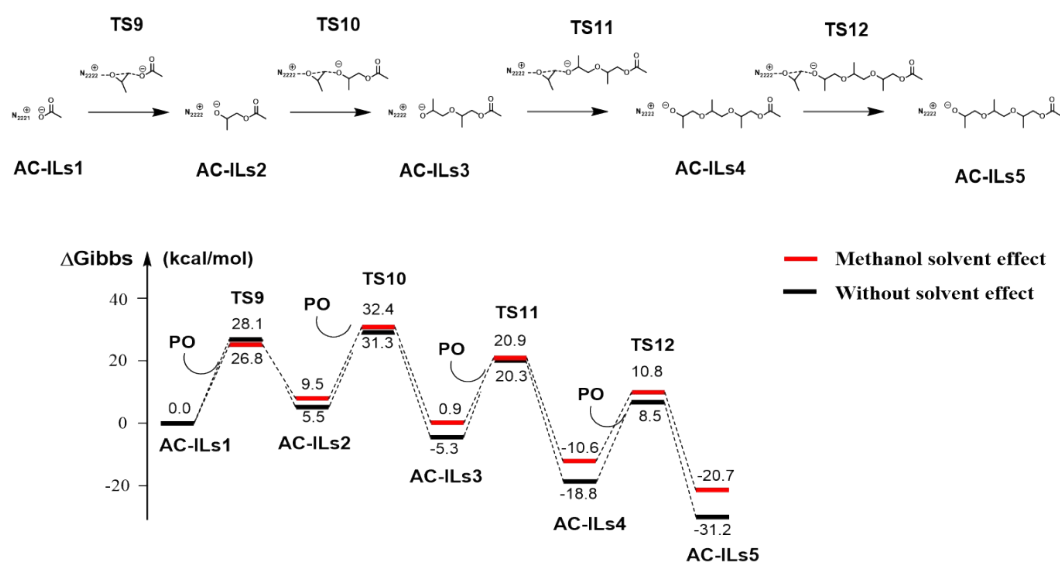


Figure S7: Potential energy profiles for the coupling reaction between AC-ILs and PO. Red line represents methanol solvent effect as black for without solvent effect.

3) Reaction mechanism of coupling reaction of PO with methanol under AC-IL_n catalysts

The ring-opening of PO is promoted both the electrophilic attack of the H atom from [N₂₂₂₂] and the nucleophilic attack from [AC] to form transition state (TS9). After cleavage of C-O, C atom from PO bond to O atom from [AC] as an intermediate (AC-ILs2) which can further electrophilic and nucleophilic attack on PO following the above steps with series transition states (TS10, TS11, TS12) and intermediates (AC-ILs3, AC-ILs4, AC-ILs5) (Figure S8a). The reaction pathway has a lower energy barrier of each ring-opening steps in methanol solvent because of the hydrogen-bond donor surroundings that methanol provided. Compared with methanol effect, the reaction is more favorable in thermodynamics due to the stable intermediates without solvent effect (Figure S8b).

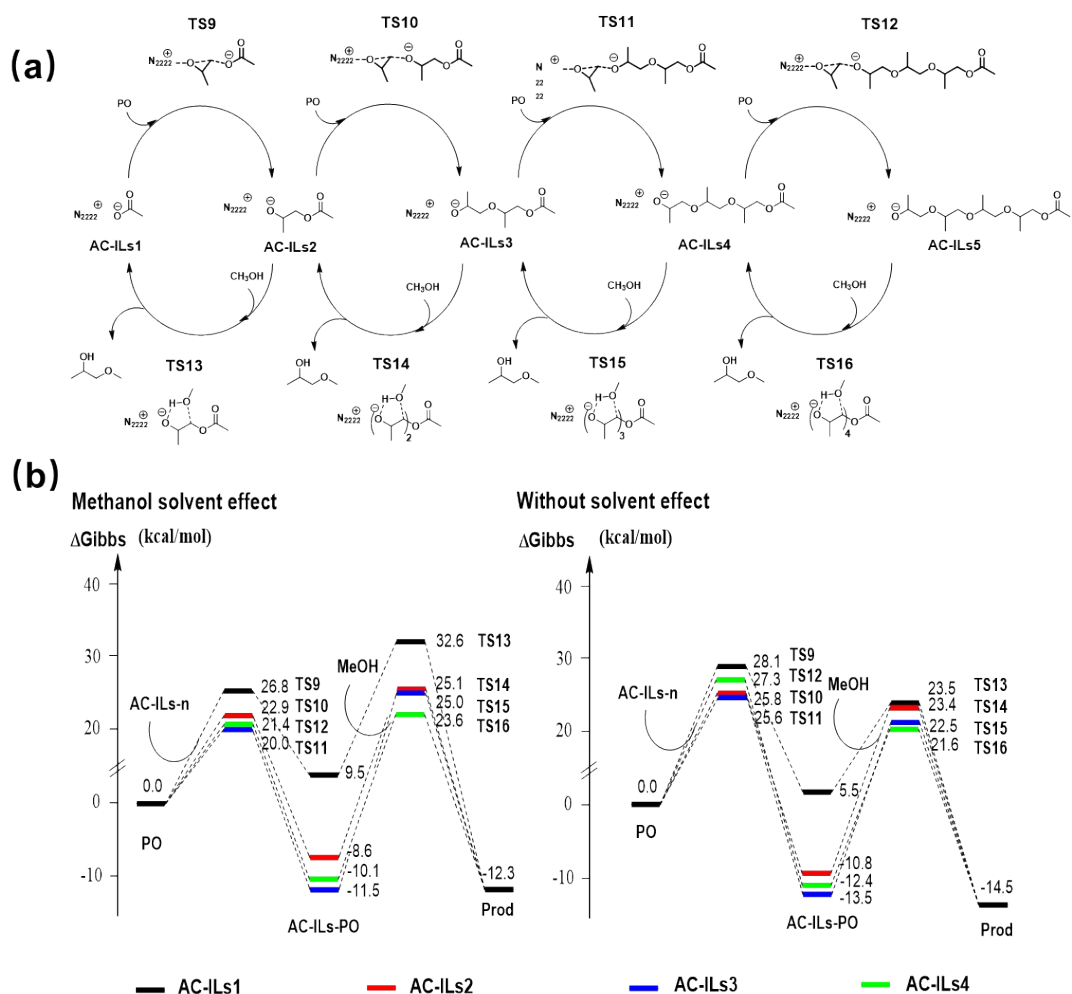


Figure S8: (a) Reaction pathway with transition states and intermediates catalyzed by AC-ILs1, (b) Potential energy profiles for the coupling reaction catalyzed by AC-ILsn (n=1,2,3,4)

4. General procedure for coupling reaction between PO and CH₃OH

Batch flow: The catalytic experiments were carried out in a 100ml autoclave reactor. PO, CH₃OH and catalysts (PO 0.25 mol, CH₃OH 0.75 mol, CAT 0.25 mmol) were introduced into reactor (100 ml). After running at 120 °C for 1 h, the reactor was cooled down to room temperature with the product analyzed by a gas chromatograph with FID.

PO flow: The catalytic experiments were carried out in a 100 ml autoclave reactor. Methanol (0.75 mol) and catalysts (0.25 mmol) were introduced into reactor. During running at 120 °C for 1h, 0.25mol PO would enter into reactor with different flow (0.25 mol/h, 0.5 mol/h, 0.75 mol/h, 1.5 mol/h). After the introduction of PO in different time (60 min, 30 min, 20 min, 10

min), the reaction would further carried on until 1 h. The reactor was cooled down to room temperature with the product analyzed by a gas chromatograph with FID.

Methanol flow: The catalytic experiments were carried out in a 100ml autoclave reactor. PO (0.25 mol) and catalysts (0.25 mmol) were introduced into reactor. During running at 120 °C for 1 h, 0.75 mol methanol would enter into reactor in different flow (0.75 mol/h, 1.5 mol/h, 2.25 mol/h, 4.5 mol/h). After the introduction of methanol within different time (60 min, 30 min, 20 min, 10 min), the reaction would continue until 1 h. The reactor was cooled down to room temperature with the product analyzed by a gas chromatograph with FID.

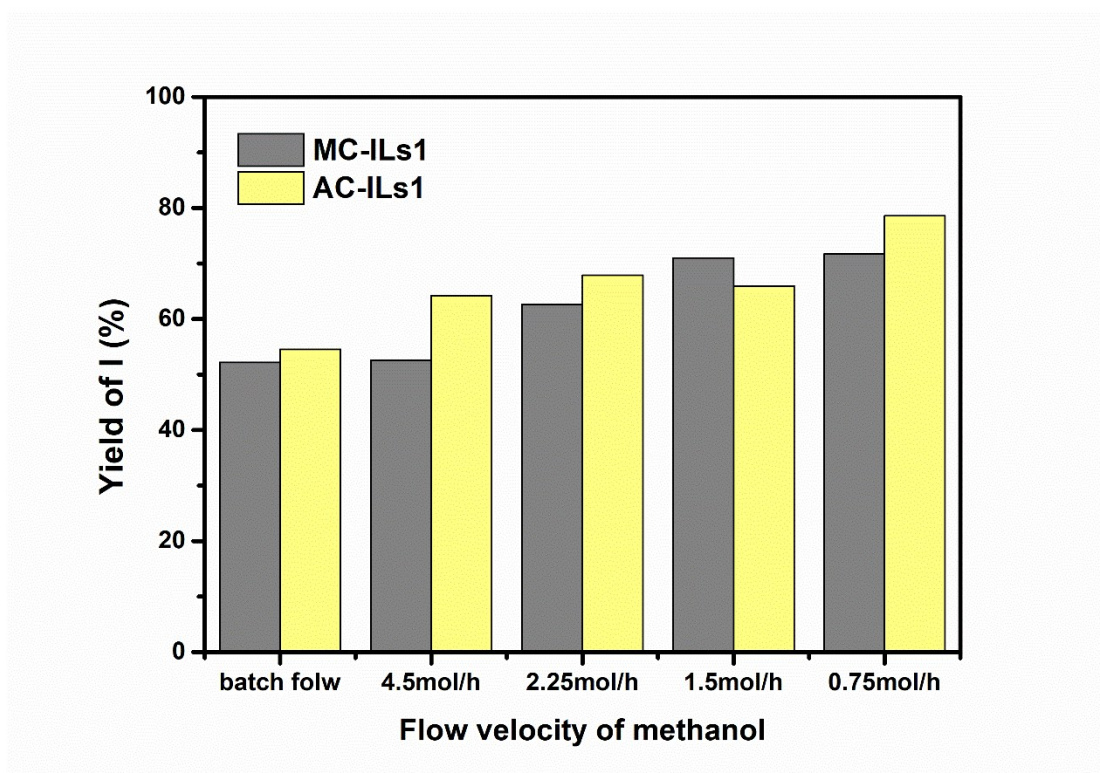


Figure S9: Catalytic performance of MC-ILs1(Gray column), AC-ILs1(Yellow column) tested by methanol flow feeding with different velocity.

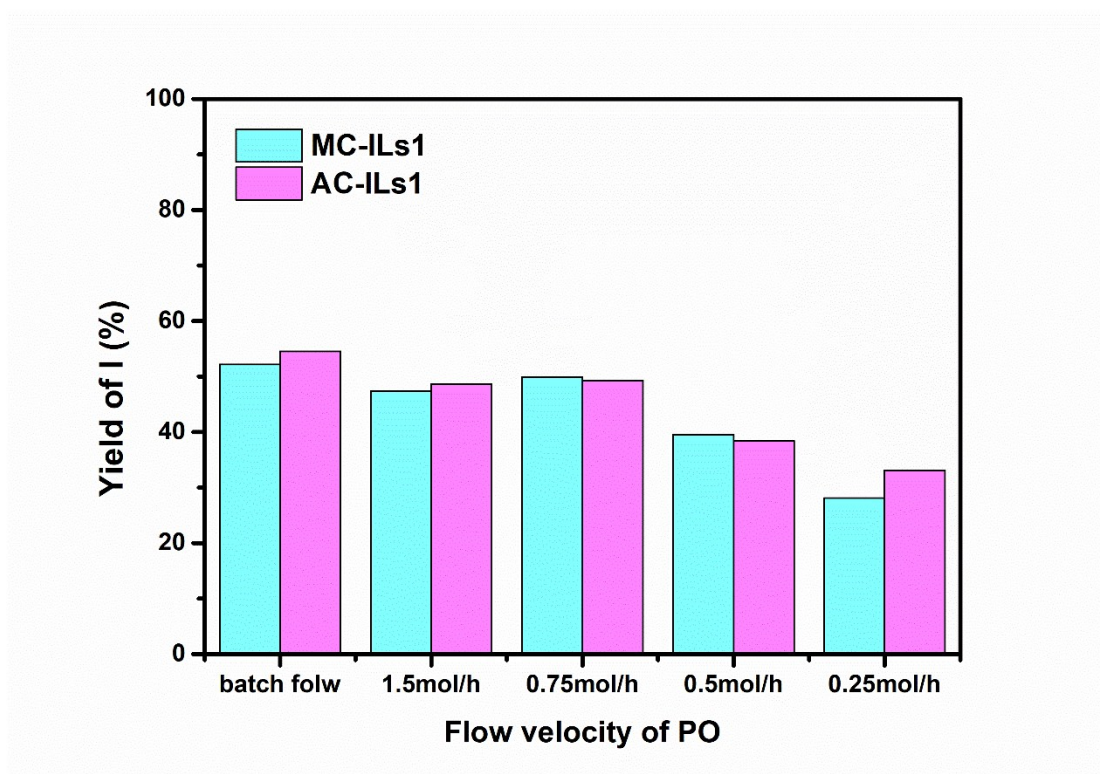


Figure S10: Catalytic performance of MC-ILs1 (Cyan column) and AC-ILs1 (Magenta column) tested by PO flow feeding with different velocity.

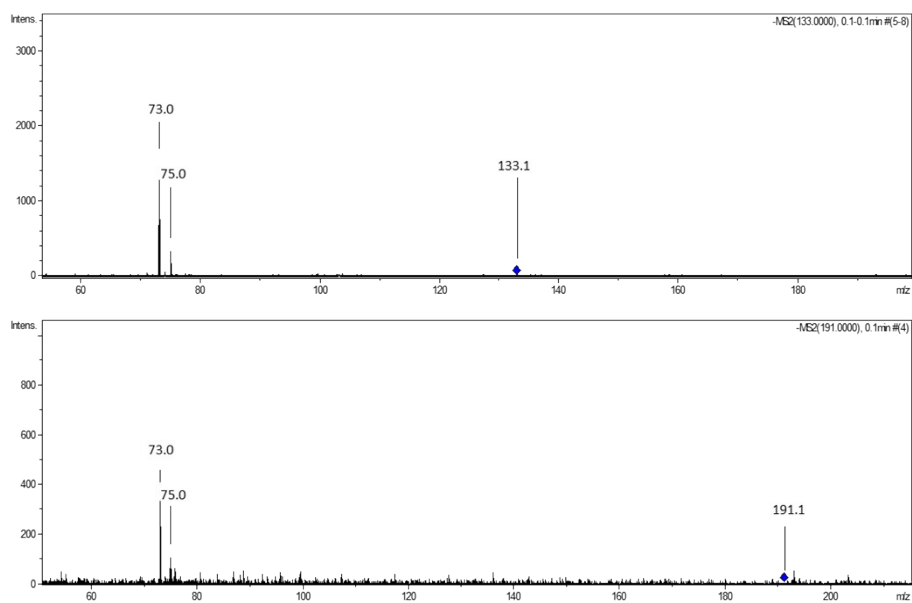


Figure S11: ESI-QTOF-MSMS of negative ion m/z 133.1 and 191.1 corresponding to MC-ILs2 and MC-ILs3